

Interatomic potentials for materials with interacting electrons

S. L. Dudarev · P. M. Derlet

Received: 21 February 2007 / Accepted: 21 March 2007 / Published online: 22 January 2008
© Springer Science+Business Media B.V. 2008

Abstract Evidence for the significant part played by magnetism in the picture of interatomic interactions in iron and iron-based alloys has recently emerged from density functional studies of the structure of radiation induced defects. In this paper we examine the range of validity of the currently available model interatomic potentials for magnetic iron, investigate the effect of electron–electron interaction on the strength of chemical bonding between atoms, follow the link between the multi-band Hubbard and the Stoner models, and review the concepts underlying the recent development of a semi-empirical magnetic interatomic potential.

Keywords Interatomic potentials · Magnetism · Molecular dynamics · Electron correlations · Iron · Magnetic potential

1 Introduction

Recent density functional calculations [1–5] have revealed a pattern of systematic qualitative differences between the structure of vacancy and self-interstitial atom defects in iron and the non-magnetic bcc metals (see Table 1).

These data show that while a highly mobile $\langle 111 \rangle$ (the $\langle 111 \rangle$ dumbbell or the $\langle 111 \rangle$ crowdion) self-interstitial atom configuration has the lowest formation energy in all the non-magnetic body-centred cubic (bcc) metals, in bcc iron it is the significantly less mobile $\langle 110 \rangle$

S. L. Dudarev (✉)

Theory and Modelling Department, Culham Science Centre, EURATOM/UKAEA Fusion Association,
Oxfordshire OX14 3DB, UK
e-mail: Sergei.Dudarev@UKAEA.org.uk

S. L. Dudarev

Department of Physics, Imperial College, Exhibition Road, London SW7 2AZ, UK

P. M. Derlet

Paul Scherrer Institute, 5232 Villigen PSI, Switzerland
e-mail: Peter.Derlet@psi.ch

Table 1 Enthalpies of formation and migration of vacancy and self-interstitial defects in body-centred cubic metals found using density functional theory in [3–5]

enthalpy (eV)	V	Nb	Ta	Cr	Mo	W	Fe
H^v	2.51	2.99	3.14	2.64	2.96	3.56	2.07
H_m^v	0.62	0.91	1.48	0.91	1.28	1.78	0.67
$H_{(111)}^v$ DB	3.367	5.253	5.832	5.685	7.417	9.548	4.45
$H_{(111)}^v$ CR	3.371	5.254	5.836	5.660	7.419	9.551	4.45
$H_{(110)}^v$	3.652	5.597	6.382	5.674	7.581	9.844	3.75
$H_{\text{tetrahedral}}^v$	3.835	5.758	6.771	6.189	8.401	11.05	4.26
$H_{(100)}^v$	3.918	5.949	7.003	6.643	9.004	11.49	4.75
$H_{\text{octahedral}}^v$	3.964	6.060	7.095	6.723	9.067	11.68	4.94

dumbbell that represents the ground state of the defect. This, as well as a significant amount of experimental information showing systematic differences between the properties of magnetic bcc iron and those of non-magnetic bcc transition metals, stimulated the development of a ‘magnetic’ semi-empirical potential for molecular dynamics simulations [6,7].

It is well known that electrons are responsible for the formation of chemical bonds, and hence it is natural to think about including electron correlation effects in the treatment of interatomic interactions, even at an empirical level of approximation. However, in the derivations of semi-empirical interatomic potentials for practical large-scale molecular dynamics simulations, electrons so far have invariably been treated as independent and non-interacting particles.

2 The tight-binding model for electron correlations

There are several fundamental points that need to be addressed in a computational scheme (‘a semi-empirical potential’) for the fast evaluation of forces acting between atoms in a transition metal, or in a transition metal alloy. We start by mapping the problem of interatomic interactions onto a tight-binding multi-band Hamiltonian (see e.g. [8,9])

$$\hat{H} = \sum_{i,j} \sum_{i \neq j} \sum_{m,m',\sigma} t_{im,jm'} \hat{c}_{im\sigma}^\dagger \hat{c}_{jm'\sigma} + \sum_{i,m,\sigma} \epsilon_i \hat{c}_{im\sigma}^\dagger \hat{c}_{im\sigma} + \sum_i \left[\frac{\bar{U}}{2} \sum_{m,m',\sigma} \hat{n}_{im,\sigma} \hat{n}_{im',-\sigma} + \frac{\bar{U} - \bar{J}}{2} \sum_{m,m',\sigma} \hat{n}_{im,\sigma} \hat{n}_{im',\sigma} (1 - \delta_{mm'}) \right]. \quad (1)$$

The t -term in this equation is the kinetic energy of quantum hopping between sites i and j , ϵ_i is the single-particle energy of an electron on site i , and the term in square brackets describes interaction between electrons on the same site i .

There is extensive literature where the authors investigate a variety of phenomena associated with the electronic structure of models described by this, or similar, Hamiltonians [10,11]. In this paper we concentrate on an entirely different aspect of the problem, which is normally not considered within a treatment based on Hamiltonian (1). We are interested in evaluating forces that interacting electrons exert on atoms forming the lattice itself, and in finding ways of eliminating the electronic degrees of freedom from the treatment of interatomic forces. Eventually we would like to derive a ‘semi-empirical interatomic potential’

suitable for multi-million molecular dynamics simulations of materials where interaction between electrons has a significant effect on mechanical properties.

By examining Hamiltonian (1), we see that a semi-empirical potential must be able to approximate three distinct effects contributing to the picture of interatomic interactions. The first is the formation of chemical bonds. They form as a result of quantum hopping of electrons or, equivalently, due to the hybridization of atomic orbitals associated with neighbouring lattice sites [12, 13]. The formation of chemical bonds is described by the t -terms in Eq. 1. A hopping (hybridization) matrix element $t_{im,jm'}$ is the amplitude of a transition between an orbital m centered on site i , and an orbital m' centered on site j . If we neglect the on-site interaction between electrons (the term in square brackets in Eq. 1), the $t_{im,jm'}$ terms in the Hamiltonian (1) will give rise to the formation of bands of electronic states. In a real-space treatment of chemical bonding between atoms in a material [13] the effects of inter-site hopping are approximated by means of a scalar (in the case of s -states) or a matrix (in the case of p , d , or f -states) recursion expansion, which is usually truncated at a relatively low level of approximation. Practical simulations require that the inter-site hopping pathways extending over large distances in the crystal lattice are not retained. Evaluating higher-order terms, which correspond to long trajectories of hopping, and involve many lattice sites, rapidly becomes computationally expensive (for example even the simplest second-moment matrix recursion treatment of interaction between a transition metal atom and its environment requires evaluating 15 separate angular-dependent matrix elements [14]). Hence there is danger that an overly accurate treatment of hopping would eliminate the very advantage that a semi-empirical molecular dynamics simulation has over its density-functional counterpart, namely its high computational speed derived from the simplicity of the method. In practice the treatment of hopping rarely goes further than the inclusion of the fourth or the sixth moment of the density of states [13].

The second phenomenon that an effective potential must describe is the effective ‘repulsion’ between atoms at short distances. In molecular dynamics the short-range repulsion, as well as all the other terms that are not taken into account in the treatment of quantum hopping, are described by either a pairwise or by a more complex many-body (especially if bond screening is included) potential [15]. To derive a semi-empirical potential, the bonding and the repulsive parts are fitted simultaneously to a set of *ab-initio* and experimentally measured parameters characterizing the material, in the hope that the overall mathematical consistency of the model would ensure that the range of validity of the resulting expression is broader than the range spanned by the data used as input for a fitting algorithm [16, 17].

The third effect that until recently received almost no attention in connection with the semi-empirical treatment of interatomic interactions, is the part played by the electron-electron interactions and magnetism. For example, the on-site electron-electron repulsion suppresses hybridization between atomic orbitals and hence weakens chemical bonds between atoms in a material [10]. This was noted in connection with the treatment of interatomic cohesion in uranium dioxide [18], and then more systematically investigated within the framework of the LSDA+U method [9]. The on-site interaction between electrons is described by the many-body term of the Hamiltonian (1). In Eq. 1 parameter \bar{U} is the Coulomb energy of repulsion between a pair of electrons with antiparallel spins occupying the same lattice site, and \bar{J} is the matrix element of *intra-atomic* exchange between the electrons. The on-site interaction part of the Hamiltonian has the form

$$\hat{H}_i = \bar{U} \sum_{m,m'} \hat{n}_{im\uparrow} \hat{n}_{im'\downarrow} + \frac{(\bar{U} - \bar{J})}{2} \sum_{m,m', m \neq m'} [\hat{n}_{im\uparrow} \hat{n}_{im'\uparrow} + \hat{n}_{im\downarrow} \hat{n}_{im'\downarrow}]. \quad (2)$$

In the absence of hopping t -terms Hamiltonian (2) describes an isolated atom. It is instructive to start by investigating its eigenstates and eigenvalues. This investigation leads to a somewhat unexpected conclusion that in the complex mathematical structure of Hamiltonian (2) only one small term is actually responsible for the spontaneous formation of the magnetic moment.

An isolated atom of iron contains seven d -electrons. These electrons occupy the 10 potentially available d -states, five states with spin up and five states with spin down. Let us assume that the seven electrons form a configuration where five electrons have spin up and the two remaining electrons have spin down. In this case the energy of an atom is

$$E = \bar{U} \cdot 5 \cdot 2 + \frac{(\bar{U} - \bar{J})}{2} (5 \cdot 4 + 2 \cdot 1) = 21\bar{U} - 11\bar{J},$$

and the total magnetic moment equals $(5 - 2)\mu_B = 3\mu_B$. We now compare this energy with the energy of a configuration where only four electrons have spin up and the remaining three electrons have spin down. The energy of this configuration is

$$E = \bar{U} \cdot 4 \cdot 3 + \frac{(\bar{U} - \bar{J})}{2} (4 \cdot 3 + 3 \cdot 2) = 21\bar{U} - 9\bar{J}.$$

The total magnetic moment is now $(4 - 3)\mu_B = 1\mu_B$. The energy of the high magnetic moment configuration is lower than the energy of the low moment configuration by the amount of $2\bar{J}$. In numerical terms, assuming that $\bar{U} = 10\text{ eV}$ and $\bar{J} = 1\text{ eV}$, we find that the total energy of the electron-electron interaction in the high-moment configuration is 199 eV while the energy of interaction between electrons in the low-moment configuration is 201 eV. The small $\sim 1\%$ difference between the two energies is entirely due to the intra-atomic exchange interaction between electrons. The much stronger direct Coulomb repulsion described by the \bar{U} term plays no part in determining the magnetic state of an atom. The fact that the configuration with the highest magnetic moment has the lowest energy is a manifestation of Hund's rule.

Generalizing this treatment to the case of an arbitrary non-integer number of electrons occupying the atom, we write

$$E = \bar{U}N_{\uparrow}N_{\downarrow} + \frac{(\bar{U} - \bar{J})}{2} [N_{\uparrow}(N_{\uparrow} - 1) + N_{\downarrow}(N_{\downarrow} - 1)].$$

To simplify this equation we introduce two new variables, the total number N of electrons per atom $N = N_{\uparrow} + N_{\downarrow}$, and the magnetic moment M of an atom $M = N_{\uparrow} - N_{\downarrow}$. The energy of an atom now is

$$\begin{aligned} E &= \bar{U} \left(\frac{N + M}{2} \right) \left(\frac{N - M}{2} \right) + \frac{\bar{U} - \bar{J}}{2} \left[\frac{1}{4}(N + M)^2 + \frac{1}{4}(N - M)^2 - N \right] \\ &= \left(\frac{\bar{U}}{4} + \frac{\bar{U} - \bar{J}}{4} \right) N^2 - \frac{\bar{U} - \bar{J}}{2} N - \frac{\bar{J}}{4} M^2 \approx \frac{\bar{U}}{2} N(N - 1) - \frac{\bar{J}}{4} M^2. \end{aligned} \quad (3)$$

The main point illustrated by this equation is that the only term that explicitly depends on the magnetic moment M of an atom is

$$E_{\text{magnetic}}(M) = -\frac{\bar{J}}{4} M^2. \quad (4)$$

The magnitude of parameter \bar{J} for a $3d$ transition metal atom is almost independent of the environment of the atom and is of the order of 1 eV [19]. Comparing Eq. 4 with the

phenomenological Stoner model [13], where the energy of exchange interaction between electrons has the form

$$E_{\text{Stoner}}(M) = -\frac{I}{4}M^2, \quad (5)$$

and where I is the Stoner parameter, we see that the intra-atomic exchange parameter \bar{J} of Hamiltonian (2) is the same as the parameter I of the Stoner model. Taking this identity into account, in what follows we will be using I instead of \bar{J} in all the equations given below.

The energy of an atom (3) also contains a term $\bar{U}N(N-1)/2$ that describes direct on-site Coulomb repulsion between electrons. The interplay between this term and the hopping t -term suppresses chemical bonding in Mott insulators [9, 10, 18]. In a metal the effect of self-screening [20] reduces the strength of on-site Coulomb repulsion described by the parameter \bar{U} of Hamiltonian (1). Furthermore, the fact that in a metal the bandwidth $W \sim \sqrt{Z}|t|$, where Z is the effective number of neighbours of an atom in a lattice, is comparable or greater than \bar{U} , makes effects of on-site Coulomb repulsion less significant than in the case of a Mott insulator.

3 The Stoner Hamiltonian

To derive an approximate Hamiltonian describing the occurrence of magnetism in iron and other transition metals we introduce the operator of the total number of electrons occupying a lattice site $\hat{N}_i = \hat{N}_{i\uparrow} + \hat{N}_{i\downarrow}$ and the operator of the total magnetic moment $\hat{M}_i = \hat{N}_{i\uparrow} - \hat{N}_{i\downarrow}$ associated with this site. Using these notations we transform Hamiltonian (2) to a simpler form (we remind the reader that $\bar{J} \equiv I$)

$$\hat{H}_i = \frac{\bar{U}}{2}\hat{N}_i(\hat{N}_i - 1) - \frac{I}{4}\hat{N}_i^2 - \frac{I}{4}\hat{M}_i^2 + \frac{I}{2}\hat{N}_i. \quad (6)$$

There are two types of terms in this Hamiltonian. The terms that depend on \hat{N}_i describe charge fluctuations associated with hopping of electrons between lattice sites. On the other hand, it is the Stoner term $-I\hat{M}_i^2/4$ that is responsible for the formation of magnetic moments on individual lattice sites. In a metal we neglect fluctuations of the total number of electrons on a site (the expectation value of \hat{N}_i is kept constant by the charge neutrality condition) and effectively re-define the on-site energies ϵ_i . The only remaining ‘non-trivial’ part of Hamiltonian (6) is proportional to the square of the operator of the total magnetic moment. By retaining this magnetic term, we arrive at the Stoner Hamiltonian [21]

$$\hat{H}_{\text{Stoner}} = \sum_{i,j} \sum_{i \neq j} \sum_{m,m',\sigma} t_{im,jm'} \hat{c}_{im\sigma}^\dagger \hat{c}_{jm'\sigma} + \sum_{i,m,\sigma} \epsilon_i \hat{c}_{im\sigma}^\dagger \hat{c}_{im\sigma} - \frac{I}{4} \sum_i \hat{M}_i^2 \quad (7)$$

Due to the operator form of the magnetic Stoner term, this Hamiltonian is expected to be of similar complexity to the Hubbard Hamiltonian [11]. At the same time the physical picture described by the Stoner Hamiltonian (7) is completely different to that of the Hubbard Hamiltonian. The derivation given above shows that the Stoner parameter I in Eq. 7 describes intra-atomic exchange. It bears no relation to the direct Coulomb interaction between electrons described by the U -term of the conventional single-band Hubbard model [11].

The ground states of Hamiltonian (7) for perfect bcc and fcc lattices, as well as for the case of bcc lattice containing a defect, were recently investigated by Liu et al. [22] in

the mean-field approximation. One of the remarkable findings of [22] is the demonstration of the fact that a mean-field solution is able to reproduce the antiferromagnetic ordering of moments in the core of an interstitial defect found earlier in density functional calculations [1].

The tight-binding mean-field approximation adopted in [22] is suitable for the treatment of a relatively small system containing no more than a thousand atoms. How do we extend the treatment to a significantly larger system? Consider a trial wave function Ψ describing an electronic configuration for an arbitrary set of coordinates of atoms $\mathbf{R}_1, \mathbf{R}_2, \dots, \mathbf{R}_N$, which has corresponding expectation values of local magnetic moment labeled as $\mathbf{M}_1, \mathbf{M}_2, \dots, \mathbf{M}_N$. The Stoner Hamiltonian (7) is invariant with respect to the rotation of the direction of quantization of the total magnetic moment, and hence the expectation value of energy $\langle \Psi | \hat{H}_{\text{Stoner}} | \Psi \rangle$ must be invariant with respect to the choice of this quantization axis. A sufficiently general form of a function of coordinates of atoms and expectation values of magnetic moments that is independent of the choice of the direction of the quantization axis is

$$\begin{aligned} E(\mathbf{R}_1, \mathbf{R}_2, \dots, \mathbf{R}_N; \mathbf{M}_1, \mathbf{M}_2, \dots, \mathbf{M}_N) &= \langle \Psi | \hat{H}_{\text{Stoner}} | \Psi \rangle \\ &= E^{(0)}(\mathbf{R}_1, \mathbf{R}_2, \dots, \mathbf{R}_N) + \sum_i E_i^{(1)}(\mathbf{R}_1, \mathbf{R}_2, \dots, \mathbf{R}_N) \mathbf{M}_i^2 \\ &\quad + \sum_i E_i^{(2)}(\mathbf{R}_1, \mathbf{R}_2, \dots, \mathbf{R}_N) (\mathbf{M}_i^2)^2 + \sum_{i,j,i \neq j} E_{ij}^{(3)}(\mathbf{R}_1, \mathbf{R}_2, \dots, \mathbf{R}_N) \mathbf{M}_i \cdot \mathbf{M}_j + \dots \end{aligned} \quad (8)$$

In principle, this expansion contains an infinite number of terms involving even powers of magnetic moments, as well as scalar products of moments associated with different lattice sites.

By minimizing the energy $E(\mathbf{R}_1, \mathbf{R}_2, \dots, \mathbf{R}_N; \mathbf{M}_1, \mathbf{M}_2, \dots, \mathbf{M}_N)$ with respect to the *magnitude* of magnetic moments $|\mathbf{M}_1|, |\mathbf{M}_2|, \dots, |\mathbf{M}_N|$ (note that this minimization only requires redistributing electrons between the spin states within each atom, and does not interfere with the local charge neutrality condition), we arrive at a general formula for the energy, invariant with respect to the choice of the direction of quantization axis for magnetic moments, and characterized by the positions of atoms $\mathbf{R}_1, \mathbf{R}_2, \dots, \mathbf{R}_N$ and the directions of unit vectors of magnetic moments $\mathbf{e}_1, \mathbf{e}_2, \dots, \mathbf{e}_N$, namely

$$\begin{aligned} E(\mathbf{R}_1, \mathbf{R}_2, \dots, \mathbf{R}_N; \mathbf{e}_1, \mathbf{e}_2, \dots, \mathbf{e}_N) &= U(\mathbf{R}_1, \mathbf{R}_2, \dots, \mathbf{R}_N) \\ &\quad - \frac{1}{2} \sum_{i \neq j} J_{ij}(\mathbf{R}_1, \mathbf{R}_2, \dots, \mathbf{R}_N) \mathbf{e}_i \cdot \mathbf{e}_j + \dots \end{aligned} \quad (9)$$

Functions $U(\mathbf{R}_1, \mathbf{R}_2, \dots, \mathbf{R}_N)$ and $J_{ij}(\mathbf{R}_1, \mathbf{R}_2, \dots, \mathbf{R}_N)$ depend on the positions of atoms and parameters of the Stoner Hamiltonian (7). In principle they can be evaluated using a suitable approximation for the trial wave function Ψ . In a ferromagnetic configuration, where all the moments are parallel to each other, and where $\mathbf{e}_i \cdot \mathbf{e}_j = 1$ for all i and j , energy (9) depends only on coordinates of atoms, and is subject to a constraint that the magnitude of each magnetic moment is determined by the condition that the total energy (8) is minimum. This limiting case of a ferromagnetically ordered (but geometrically arbitrarily distorted) atomic configuration was investigated in [6, 7] and led to the development of a ‘magnetic’ interatomic potential. We now briefly review this approach.

4 The semi-empirical magnetic potential

4.1 Formalism

Consider the one-particle terms of Hamiltonians (1) or (7)

$$\hat{H}_{one-particle} = \sum_{i,j, i \neq j} \sum_{m,m',\sigma} t_{im,jm'} \hat{c}_{im\sigma}^\dagger \hat{c}_{jm'\sigma} + \sum_{i,m,\sigma} \epsilon_i \hat{c}_{im\sigma}^\dagger \hat{c}_{im\sigma}. \quad (10)$$

These terms describe hopping of electrons between sites i and j , as well as the on-site energies of the electrons. These terms are diagonal with respect to the spin index of electrons. Hence Hamiltonian (10) can be written in the form of a square matrix

$$H_{im,jm'} = \epsilon_i \delta_{im,jm'} + t_{im,jm'}.$$

The eigenvalues E_α of this matrix $H_{im,jm'}$ are found by a unitary transformation $C_{im,\alpha}$

$$E_\alpha \delta_{\alpha\alpha'} = \sum_{im,jm'} C_{\alpha,im}^\dagger [\epsilon_i \delta_{im,jm'} + t_{im,jm'}] C_{jm',\alpha'}.$$

Using these eigenvalues we define the projected on-site density of states $D_i(E)$

$$D_i(E) = \sum_{\alpha,m} |C_{im,\alpha}|^2 \delta(E - E_\alpha). \quad (11)$$

In a perfect crystal where all the sites are equivalent, the projected density of states is independent of site index i . Taking the on-site energy $\epsilon_i \equiv \epsilon$ as the origin of the energy axis, we write the total energy of the electrons as

$$E_{tot} = 2 \int_{-\infty}^{\epsilon_F} E D(E) dE.$$

By assuming that the system is ferromagnetically ordered, adding the Stoner term to this equation and noting that it may change the relative occupation numbers of the spin up and spin down states, we write the total energy of an atom as

$$E_{tot} = \int_{-\infty}^{\epsilon_{F\uparrow}} E D(E) dE + \int_{-\infty}^{\epsilon_{F\downarrow}} E D(E) dE - IM^2/4. \quad (12)$$

Here

$$M = \int_{-\infty}^{\epsilon_{F\uparrow}} D(E) dE - \int_{-\infty}^{\epsilon_{F\downarrow}} D(E) dE$$

is the magnetic moment of an atom. The total number of electrons occupying an atom, which in a metal remains constant due to the local charge neutrality condition, is given by

$$N = \int_{-\infty}^{\epsilon_{F\uparrow}} D(E) dE + \int_{-\infty}^{\epsilon_{F\downarrow}} D(E) dE = \text{const.} \quad (13)$$

In a self-consistent electronic structure calculation the total energy (12) is minimized using the notion of the one-particle Kohn-Sham states. The energies of these states are

$$\begin{aligned}\epsilon_{\uparrow} &= \frac{\delta E_{tot}}{D(E)\delta n_{\uparrow}(E)} = E - \frac{I}{2} \left(\int_{-\infty}^{\epsilon_{F\uparrow}} D(E)dE - \int_{-\infty}^{\epsilon_{F\downarrow}} D(E)dE \right) = E - \frac{I}{2}M \\ \epsilon_{\downarrow} &= \frac{\delta E_{tot}}{D(E)\delta n_{\downarrow}(E)} = E + \frac{I}{2} \left(\int_{-\infty}^{\epsilon_{F\uparrow}} D(E)dE - \int_{-\infty}^{\epsilon_{F\downarrow}} D(E)dE \right) = E + \frac{I}{2}M. \quad (14)\end{aligned}$$

The impression that one has from examining these equations is that the presence of magnetism results in shifting the energy bands up or down by the amount $IM/2$. The sign of the shift depends on the projection of spin. The sum of the one-particle energies

$$\begin{aligned}E' &= \int_{-\infty}^{\epsilon_{F\uparrow}} dE \left[E - \frac{I}{2}M \right] D(E) + \int_{-\infty}^{\epsilon_{F\downarrow}} dE \left[E + \frac{I}{2}M \right] D(E) \\ &= \int_{-\infty}^{\epsilon_{F\uparrow}} E D(E)dE + \int_{-\infty}^{\epsilon_{F\downarrow}} E D(E)dE - \frac{I}{2}M^2, \quad (15)\end{aligned}$$

is *not* equal to the total energy of the system. It overestimates the magnetic term by a factor of two in comparison with the original expression (12). To compensate for the error we must add to (15) the so-called double counting correction [23]

$$+ \frac{I}{4}M^2. \quad (16)$$

This correction is not small, and the fact that it has to be introduced shows that in the problem of interacting electrons the meaning of the effective energies of single-particle states given by Eq. 14 is quite limited. Furthermore, we cannot assume that in Eqs. 14 and 15 the Fermi energies for the *shifted* spin-up and spin down states have to be the same. Fig. 1 shows the variation of the total energy as a function of magnetic moment $E(M)$ evaluated using Eqs. 12–13, and Eqs. 14–15. In the latter case we took the upper limits of integration as $\epsilon_{F\uparrow} = \epsilon_F + IM/2$ and $\epsilon_{F\downarrow} = \epsilon_F - IM/2$, implying that ϵ_F is a universal Fermi energy for the *shifted* spin-up and spin-down one-particle states. A comparison between the curve found using the effective single particle states, and the exact calculation based on Eq. 12, reveals only an agreement at the maximum and the minimum of the curve, clearly demonstrating the limited applicability of the single particle picture.

Owing to this fact, in our derivation of the functional form of the magnetic potential [6, 7] we did not use the single-particle states. In the Born-Oppenheimer approximation the electronic configuration is always at the minimum of energy corresponding to a given set of atomic coordinates. Hence the task of a semi-empirical potential is to follow and to reproduce, as accurately as possible, the value and the derivatives of the total energy *at its minimum* as a function of positions of atoms in the system. Instead of introducing the system of Kohn-Sham states we minimized the energy by differentiating the Fermi energies of the spin up and spin down states [6, 7]. We found that the condition for the minimum of energy has the form

$$IM = I \int_{\epsilon_{F\downarrow}}^{\epsilon_{F\uparrow}} D(E)dE = \epsilon_{F\uparrow}(N, M) - \epsilon_{F\downarrow}(N, M). \quad (17)$$

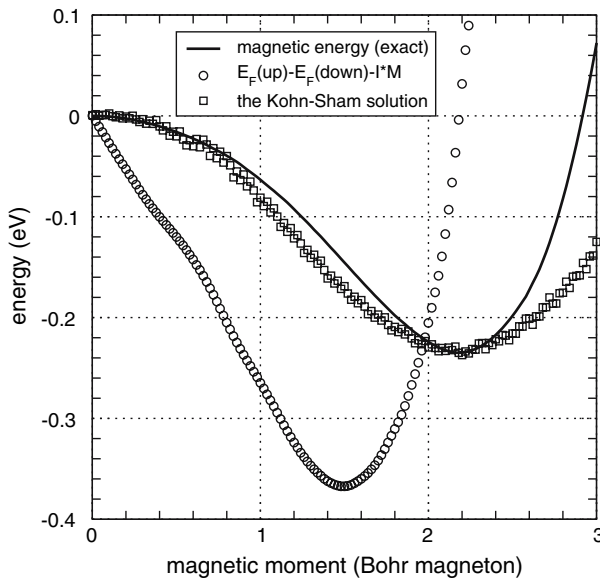


Fig. 1 Solid black line: the magnetic part of the total energy calculated numerically using Eqs. 12–13 in conjunction with an LMTO electronic density of states. Squares: the magnetic part of the total energy calculated numerically using Eqs. 14–15 and the same LMTO-derived density of states. In both cases we assumed that $I = 0.78$ eV and $N = 6.57$. Circles show the difference $\epsilon_{F\uparrow}(M) - \epsilon_{F\downarrow}(M) - IM$ plotted as a function of magnetic moment M . This line crosses the horizontal axis at the point M where the total energy is minimum

This condition is equivalent to the condition [13]

$$I\langle D(E) \rangle = 1, \quad (18)$$

where the angular brackets $\langle \dots \rangle$ denote averaging over an interval of energies between $\epsilon_{F\downarrow}$ and $\epsilon_{F\uparrow}$. Figure 1 shows that Eqs. 17 and (18) are indeed satisfied at the point where the total energy (12) is minimum.

4.2 Implementation

The development of a practical implementation of the above formalism was assisted by the realization of the fact that the exact magnetic energy treated as a function of magnetic moment (Fig. 1) can be sufficiently well described by a fourth order polynomial [6,7]:

$$E_{\text{magnetic}} = \alpha M^2 + \beta M^4. \quad (19)$$

Here the quadratic term, in which α can be either positive or negative, drives the Stoner instability and the formation of magnetic moments on an atom, whilst the positive quartic term prevents the runaway divergence of energy as a function of magnetic moment M in a magnetic configuration. The double well structure inherent in Eq. 19 is the hallmark of the Ginzburg-Landau formalism [24] that is used extensively in phenomenological studies of phase transitions. Indeed as $\alpha \rightarrow 0$, the double well structure of Eq. 19 vanishes with the corresponding loss of (in this case) ferromagnetism.

Within this simple picture, the parameters α and β depend on the local environment of the atom thus affecting the location of the symmetric double well minima defined by the equilibrium ferromagnetic moment value

$$M = \pm \sqrt{-\frac{\alpha}{2\beta}}, \quad (20)$$

and the corresponding ferromagnetic energy

$$E_{\text{magnetic}} = -\frac{\alpha^2}{4\beta}. \quad (21)$$

As in the exact case, the environmental dependence of the functional form of the magnetic energy versus magnetic moment will depend on how the local density of states responds to changes in the local atomic environment—as defined by the equilibrium solution to Eqs. 12 and 13. The practical significance of the Ginzburg-Landau approximation Eq. 19 is that only a simplified local density of states model is needed to produce the necessary leading order quadratic and quartic dependencies of the magnetic energy with respect to the magnetic moment. This constitutes an important observation since it implies that the fine details in the *d*-band density of states derived from *ab-initio* or tight binding methods do not play a defining role in the nature of ferromagnetism in bcc Fe. As we shall see, it is only the most general features of the *d*-band density of states that become important.

How simple can the functional form of the density of states for the modelling of ferromagnetism be? Previous studies have shown [6, 25, 26] that a simple rectangular density of states will produce only a quadratic term in the magnetic moment for the magnetic energy, leading to a so-called ‘flat band’ magnetism that results in a fully-saturated magnetic moment. Such a model may well describe metals such as ferromagnetic fcc Ni, however for un-saturated ferromagnetic systems such as bcc Fe it is clearly insufficient. In the development of the magnetic potential, the choice of an inverted parabolic density of states in the vicinity of the non-magnetic Fermi energy turned out to produce the needed quadratic and quartic magnetic terms. In retrospect, this is a somewhat intuitive result since such a form most simply models the large peak at the Fermi energy seen in the *ab-initio* and experimentally derived *d*-band density of states for bcc Fe.

The environmental dependence of the inverted parabolic density of states is most easily modeled via the Finnis-Sinclair second moment approximation [27, 28], where the width of the density of states is proportional to the square root of the local electronic density, ρ . The combined approximations of the inverted parabolic density of states and the second-moment environmental dependence lead then directly to

$$\alpha \propto (\sqrt{\rho_c} - \sqrt{\rho}) \quad (22)$$

and

$$\beta \propto \left(\frac{3}{4} \sqrt{\rho_c} - \sqrt{\rho} \right), \quad (23)$$

where ρ_c represents some critical local electron density at which ferromagnetism is completely suppressed. Thus the model has within it the natural feature that under compression the magnetic moment decreases continuously following Eq. 20, with a corresponding reduction in the magnetic energy (21) until a critical volume per atom is reached at which ferromagnetism vanishes. Substitution of Eqs. 22 and 23 into (20) and 21 then provide the basis from which an empirical model for ferromagnetism is derived [6].

The analysis given above addressed the fundamental aspects of the concept of magnetic interatomic potential. A detailed description of the derivation of the functional form of the potential for molecular dynamics simulations of iron is given in [6, 7]. The potential tabulated in [6, 7] was fitted to a range of properties of magnetic bcc iron, as well as to the energies of

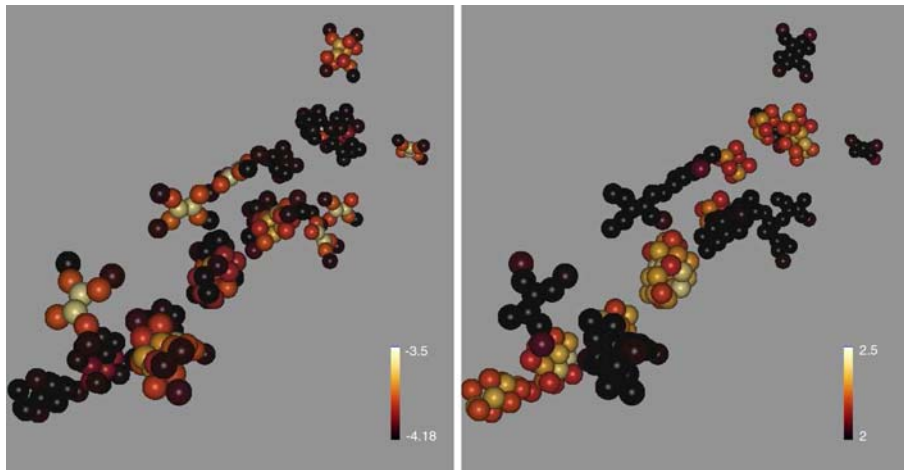


Fig. 2 Interstitial and vacancy defects produced in a collision cascade in bcc Fe. The energy of the primary knock-on atom initiating the cascade is 5 keV. In the configuration shown on the left the colour scheme refers to the potential energy of atoms forming the defects. In the right panel colour refers to the magnetic moment of an atom. Both panels show atoms the potential energy of which exceeds -4.18 eV. Comparing the structures shown in both panels we see that while the energy of atoms forming defects of both vacancy and interstitial type varies within similar range (left panel), the magnetic moments of atoms forming vacancy defects are systematically greater than the magnetic moments of atoms forming interstitial defects (right panel)

vacancy and self-interstitial atom defects. It is just as easy to use and its numerical implementation is just as fast as that of any other semi-empirical potential. An additional benefit that a magnetic potential offers to a user is its ability to evaluate, *at no extra cost*, the magnitude of the local magnetic moment on every atom in a simulation cell. Figure 2 gives an example of an application of the magnetic potential to the analysis of the *magnetic* structure of defects produced in a collision cascade in bcc Fe. Simulations of amorphous iron carried out using the magnetic potential show the formation of complex patterns of magnetic ordering related to the distribution of local strain in the material [29].

5 Conclusions

So far the potential has been developed and fitted only for the case of pure iron, and the tests carried out so far show that it performs reasonably well in simulations of defect structures and dislocations. We are of the opinion that the work done so far has only scratched the surface of the fundamental problem of large-scale atomistic simulations of systems where electrons forming chemical bonds between atoms are treated as interacting particles. Further work is required to address the unusual behaviour exhibited by many materials, including magnetic alloys, where *d*- and *f*-electrons contribute to, and in some case strongly affect, bonding between the atoms.

Acknowledgements The authors would like to thank Prof. A. P. Sutton and Prof. C. H. Woo many stimulating discussions. This work was supported by the UK Engineering and Physical Sciences Research Council, by EURATOM, and by EXTREMAT integrated project under contract number NMP3-CT-2004-500253.

References

1. Domain, C., Becquart, C.S.: *Phys. Rev. B* **65**, 024103–024114 (2001)
2. Han, S., Zepeda-Ruiz, L.A., Ackland, G.J., Car, R., Srolovitz, D.J.: *Phys. Rev. B* **66**, 220101–220104 (2002)
3. Fu, C.-C., Willaime, F., Ordejón, P.: *Phys. Rev. Lett.* **92**, 175503–175504 (2004)
4. Willaime, F., Fu, C.-C., Marinica, M.C., Dalla Torre, J.: *Nuc. Inst. Meth. B* **228**, 92–99 (2005)
5. Nguyen-Manh, D., Horsfield, A.P., Dudarev, S.L.: *Phys. Rev. B* **73**, 020101–020104 (2006)
6. Dudarev, S.L., Derlet, P.M.: *J. Phys. Condens. Matter* **17**, 7097–7118 (2005); *ibid* **19**, 239001 (2007)
7. Derlet, P.M., Dudarev, S.L.: *Prog. Mater. Sci.* **52**, 299–318 (2007)
8. Kotani, A., Yamazaki, T.: *Prog. Theor. Phys. Suppl.* **108**, 117–131 (1992)
9. Dudarev, S.L., Botton, G.A., Savrasov, S.Y., Humphreys, C.J., Sutton, A.P.: *Phys. Rev. B* **57**, 1505–1509 (1998)
10. Fulde, P.: *Electron Correlations in Molecules and Solids*, 3rd edn. Springer, Berlin (1995)
11. Fazekas, P.: *Electron Correlations and Magnetism*. World Scientific, Singapore (1999)
12. Sutton, A.P., Finnis, M.W., Pettifor, D.G., Ohta, Y.: *J. Phys. C: Solid State Phys.* **21**, 35–66 (1988)
13. Pettifor, D.G.: *Bonding and Structure of Molecules and Solids*. Oxford University Press, Oxford (1996)
14. Dudarev, S.L.: *J. Phys.: Condens. Matter* **18**, S447–S461 (2006)
15. Nguyen-Manh, D., Vitek, V., Horsfield, A.P.: *Prog. Mater. Sci.* **52**, 255–298 (2007)
16. Finnis, M.W.: *Interatomic Forces in Condensed Matter*. Oxford University Press, Oxford (2003)
17. Frederiksen, S.L., Jacobsen, K.W., Brown, K.S., Sethna, J.P.: *Phys. Rev. Lett.* **93**, 165501–165504 (2004)
18. Dudarev, S.L., Nguyen-Manh, D., Sutton, A.P.: *Philos. Mag. B* **75**, 613–628 (1997)
19. Gunnarsson, O.: *J. Phys. F: Metal Phys.* **6**, 587–606 (1976)
20. Solov'yev, I.V., Imada, M.: *Phys. Rev. B* **71**, 045103 (2005)
21. Hasegawa, H., Finnis, M.W., Pettifor, D.G.: *J. Phys. F: Metal Phys.* **15**, 19–34, see equations (2.5)–(2.7) (1985)
22. Liu, G., Nguyen-Manh, D., Liu, B.-G., Pettifor, D.G.: *Phys. Rev. B* **71**, 174115 (2005)
23. Pickett, W.E.: *J. Korean Phys. Soc.* **29**, S70–S74 (1996)
24. Landau, L.D., Lifshitz, E.M.: *Statistical Physics*, 3rd edn. Pergamon Press, Oxford (1977)
25. Pettifor, D.G.: *J. Magn. Magn. Mater.* **15–18**, 847–852 (1980)
26. Ackland, G.J.: *J. Nucl. Mater.* **351**, 20–27 (2006)
27. Finnis, M.W., Sinclair, J.E.: *Philos. Mag.* **50**, 45–55 (1984)
28. Ackland, G.J., Finnis, M.W., Vitek, V.: *J. Phys.* **F18**, L153–L157 (1984)
29. Ma, P.W., Liu, W.C., Woo, C.H., Dudarev, S.L.: *J. Appl. Phys.* **101**, 073908 (2007)